International Journal of Nanoelectronics and Materials
*Volume 13, No. 1, Jan 2020* [189-198]

# Designs and Simulations of Millimetre Wave On-chip Single Turn Inductors for 0.13 $\mu$m RF CMOS Process Technology

Hao Wuang Leong[1,2]*, Kim Ho Yeap[2] and Yee Chyan Tan[2]

[1] *Centre for VLSI Research, Universiti Tunku Abdul Rahman, Jalan Universiti, Bandar Barat, 31900 Kampar, Perak. Malaysia.*
[2] *Department of Electronic Engineering, Faculty of Engineering and Green Technology, Universiti Tunku Abdul Rahman, Jalan Universiti, Bandar Barat, 31900 Kampar, Perak. Malaysia.*

Received 11 August 2019, Revised 24 December 2019, Accepted 9 January 2020

**ABSTRACT**

*The upcoming Fifth Generation (5G) network has promoted researches in integrated circuit designs and microelectromechanical systems (MEMS). Since the 5G technologies operate mainly in the millimetre wave (mm-wave) band, developing electronic components which are compatible with this frequency range is therefore necessary. This paper presents the design of four novel inductors, applied particularly in Low Noise Amplifiers (LNAs) which operate at 60 GHz to overcome the limitations of the particular Process Design Kit (PDK) in which the provided scalable inductors are characterised at a maximum frequency of 30 GHz. The design is based on Silterra's 0.13 µm radio frequency complementary metal-oxide-semiconductor (RF CMOS) process technology. The inductors use Ultra-Thick Metal (UTM) with a copper thickness of 3.3 µm. A mixture of analytical and parametric analyses is utilised in designing the four spiral inductors which can be implemented in the PDK used by the aforementioned LNA. The inductances and Q-factors across 1 GHz to 150 GHz were plotted and analysed. The results show that the four designs exhibit very good performance at 60 GHz with minimal tolerances. This paper serves as a proof-of-concept for a methodology on custom inductor design and simulations with existing PDK limitations.*

**Keywords:** Inductance, Low Noise Amplifiers, Q-Factor, RF CMOS, S-Parameters.

## 1. INTRODUCTION

Wireless communication networks are advancing toward the Fifth Generation (5G). Since the 5G technologies operate essentially in the millimetre wave (mm-wave) band, which ranges approximately from 30 to 300 GHz, there is a frantic race in the electronics industry to develop components or devices which are compatible within the frequency range.

An inductor is a passive element in an electric circuit that stores energy in its magnetic field when current passes through the device [1]. A basic on-chip spiral inductor is made up of one or more metal windings placed on top of a bulk silicon substrate with a dielectric insulator (i.e. silicon dioxide) sandwiched in between [2]. The technological advancement in the realm of micro-electromechanical systems (MEMS) has made possible the fabrication of various novel types and shapes of on-chip inductors – some of which include the solenoidal inductors [3] and the out-of-plane inductors [4], to name a few. Moreover, in the effort to improve the Q factor of the inductor and as a protection against loss, a patterned ground shield of various configurations and designs have been studied and implemented [5]–[8].

*Corresponding author: *420lemao@1utar.my*

The performance of an inductor is assessed based on its inductance, quality factors or Q-factors (either at a specific frequency or in a specific range of frequencies) as well as its dimensions. It is worthwhile to note that the selection of an appropriate Process Design Kit (PDK) when designing an inductor is also important to ensure that the specifications used for the inductor are compatible with the circuit environment where it is intended to be implemented.

Silterra's 0.13 $\mu$m PDK, specifically CL130G (previously named C130G), has been widely used in the designs of radio frequency complementary metal-oxide-semiconductor (RF-CMOS) devices [8]–[17]. While the PDK (as of version April 2018) has built-in scalable spiral inductors toolkit which can estimate the intended inductance and Q-factors based on their dimensions and target frequency, it could not synthesise inductors of below 110 pH beyond 30 GHz. Inductances at this range are particularly useful for Low Noise Amplifiers (LNAs) which operate in mm-wave. In order to allow this PDK to be applicable in the design of mm-wave devices, therefore, it is necessary to develop inductors with inductances within this range. This paper provides a detail illustration of the designs of four novel inductors with inductances below 110 pH. As can be seen in the subsequent sections, the inductors perform very well when incorporated with LNAs operating at 60 GHz.

## 2. INDUCTORS IN A V-BAND LOW NOISE AMPLIFIER

One of the most popular methods in designing inductors operating in the mm-wave band is by using transmission lines [1], [17]. However, a straight transmission line may be infeasible to be fitted into the floorplan of an integrated circuit (IC) chip. In order to overcome this limitation, IC designers have employed spiral lines to reduce the overall length of the inductor while retaining its effective inductance. The inductance of a spiral inductor is dictated by the number of turns of the spirals – the higher the number of turns, the higher is its inductance. As a result, the inductor may occupy a large overall area if a high inductance is required. For spiral inductors operating in the mm-wave band, particularly those within the V-band (40 GHz to 75 GHz), spiral lines with either single or half turn is often sufficient. Despite spiral inductors are found to be capable of exhibiting high inductances when they are to be incorporated into circuits that operate in the mm-wave frequencies which will reduce the operating frequency, the designs are still possible to be implemented in such frequency range [1]. As can be observed in Figure 1, four inductors are needed for a 60 GHz cascode LNA designed using Silterra's 0.13 $\mu$m RF CMOS PDK [17]. The inductances of $L_p$, $L_s$, $L_g$ and $L_d$ are 68 pH, 75 pH, 84.7 pH and 104 pH, respectively. This paper mainly focuses on the design and simulations of these four targeted inductors.

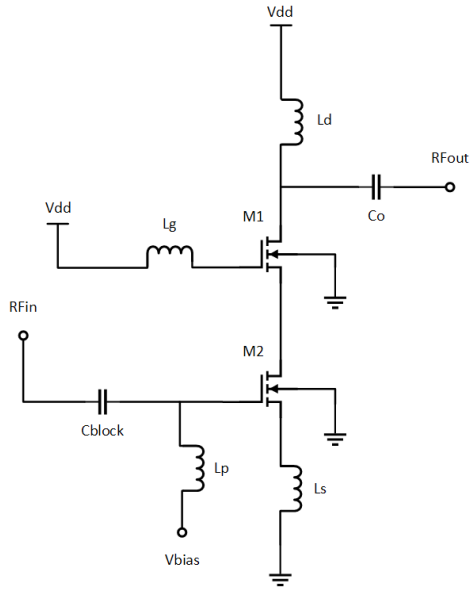


**Figure 1.** Schematic of a 60 GHz cascode LNA using gain boosting technique [17].

## 3. DESIGN

The process of designing the four targeted inductors involves two essential stages. In the first design stage, the sizes of the inductors are theoretically estimated via parametric analysis. The values obtained from the analysis are then iteratively refined and verified via simulation in the second stage. Since the Sonnet Suites™ applies a modified method of moments analysis [18] when solving computationally for the electromagnetic fields, the solutions obtained from the tool agree exceptionally well with the measurement results [19]–[24]. Hence, the Sonnet Suites™ have been used for the verification of the designs.

The relationship between the inductance and the radii of the spiral lines can be estimated based on Equation (1) below [25]:

$$L = \frac{\mu_0 \mathrm{n}^2 d_{\mathrm{avg}} c_1}{2}\left[\ln\left(\frac{c_2}{\rho}\right) + c_3\rho + c_4\rho^2\right] \quad (1)$$

Where $\mu_0$ is the permeability of free space, n is the number of turns of the spiral inductor, $d_{\mathrm{avg}}$ is the average diameter of the inductor and $\rho$ is the fill ratio. For a circular spiral inductor, the coefficients of current sheet expressions $c_1$, $c_2$, $c_3$ and $c_4$ are 1, 2.46, 0 and 0.2, respectively [17]. The parameters $d_{\mathrm{avg}}$ and $\rho$ are given in Equation (2) and Equation (3) as follows [25]:

$$d_{\mathrm{avg}} = r_{\mathrm{out}} + r_{\mathrm{in}} \quad (2)$$

$$\rho = \frac{r_{\mathrm{out}} - r_{\mathrm{in}}}{r_{\mathrm{out}} + r_{\mathrm{in}}} \quad (3)$$

Where $r_{\mathrm{in}}$ and $r_{\mathrm{out}}$ are the inner and outer radii of the spiral lines, respectively. The inductors were metallised at Ultra-Thick Metal (UTM) layer. According to Silterra's CL130G PDK, the copper thickness of the UTM is 3.3 µm and the width must be at least 2.5 µm. For ease of fabrication, a width of 5 µm has been set for the spiral lines. Therefore, the difference between $r_{\mathrm{in}}$ and $r_{\mathrm{out}}$ is 5 µm.

Since Equation (1) is in transcendental form, the solution for the radii of the spiral line (i.e. $r_{\text{in}}$ and $r_{\text{out}}$ in $\rho$) for a given inductance cannot be solved directly from the equation. To correlate the size of the spiral line and its inductance value, the inner radius of the line is arbitrarily varied at a step size of 0.5 μm. These parameters are then substituted into Equation (1) to obtain their respective inductance values L. To validate the accuracy of Equation (1), the spiral inductors with the same sizes as those used in Equation (1) are subsequently simulated in the Sonnet Suites™. Figure 2 depicts both curves which are obtained via theoretical computation and simulation, at L ranges from 60 to 110 pH. Despite minor discrepancies observed, both curves are found to be in good agreement. Figure 2 also shows that the inductance increases linearly with the inner radius of the inductors. The curves indicate that an inductor with a higher inductance value will require a larger size and vice versa.

A comparison between the parameters at the targeted inductance range (i.e. above 62 pH and below 109 pH) is illustrated in Table 1 and Figure 2. The percentage of error for inductance obtained from Equation (1) has a maximum value of 4.291%, further corroborating the high accuracy of the equation. Upon close inspection on Table 1, it is apparent that the inner radii of the targeted inductances, respectively 68 pH, 75 pH, 84.7 pH and 104 pH, fall within the ranges of 15 μm to 15.5 μm, 17 μm to 17.5 μm, 19 μm to 19.5 μm and 23.5 μm to 24 μm, respectively. To obtain the final parameter of the targeted inductances, the sizes of the spiral lines are refined by carefully adjusting them within these ranges in the Sonnet Suites™.

**Table 1** Relationship between inner radius and inductances at 60 GHz

| **Inner radius ($\mu$m)** | **Inductance (pH) computed using (1)** | **Inductance (pH) obtained from Sonnet at 60 GHz** | **Error (%)** |
|---|---|---|---|
| 16.0 | 67.5416 | 70.57 | 4.291 |
| 16.5 | 69.9993 | 72.79 | 3.834 |
| 17.0 | 72.4736 | 74.64 | 2.902 |
| 17.5 | 74.9641 | 77.40 | 3.147 |
| 18.0 | 77.4705 | 77.88 | 0.526 |
| 18.5 | 79.9922 | 81.48 | 1.826 |
| 19.0 | 82.5290 | 83.91 | 1.646 |
| 19.5 | 85.0805 | 85.61 | 0.619 |
| 20.0 | 87.6463 | 87.87 | 0.255 |
| 20.5 | 90.2262 | 89.86 | 0.408 |
| 21.0 | 92.8198 | 92.20 | 0.672 |
| 21.5 | 95.4268 | 94.38 | 1.109 |
| 22.0 | 98.0470 | 95.74 | 2.410 |
| 22.5 | 100.6800 | 100.40 | 0.279 |
| 23.0 | 103.3260 | 101.30 | 2.000 |
| 23.5 | 105.9840 | 102.90 | 2.997 |

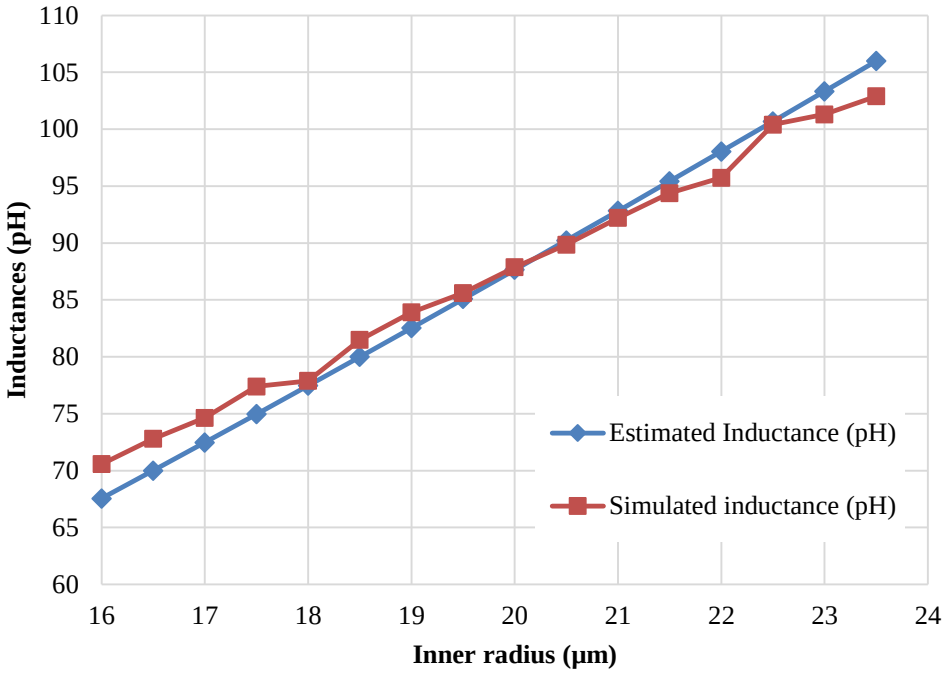


**Figure 2.** Relationship between the inner radius and both estimated and simulated inductance at 60 GHz.

## 4. RESULTS AND DISCUSSION

Figures 3 and 4 respectively show the layouts and the three-dimensional (3D) views of the four inductors. The type, order, and thickness of the material used in each structure layer, i.e. from the substrate to the passivation layer, have been carefully adjusted in order to comply with Silterra's CL130G PDK. The final parameters of the inductors are summarised in Table 2.

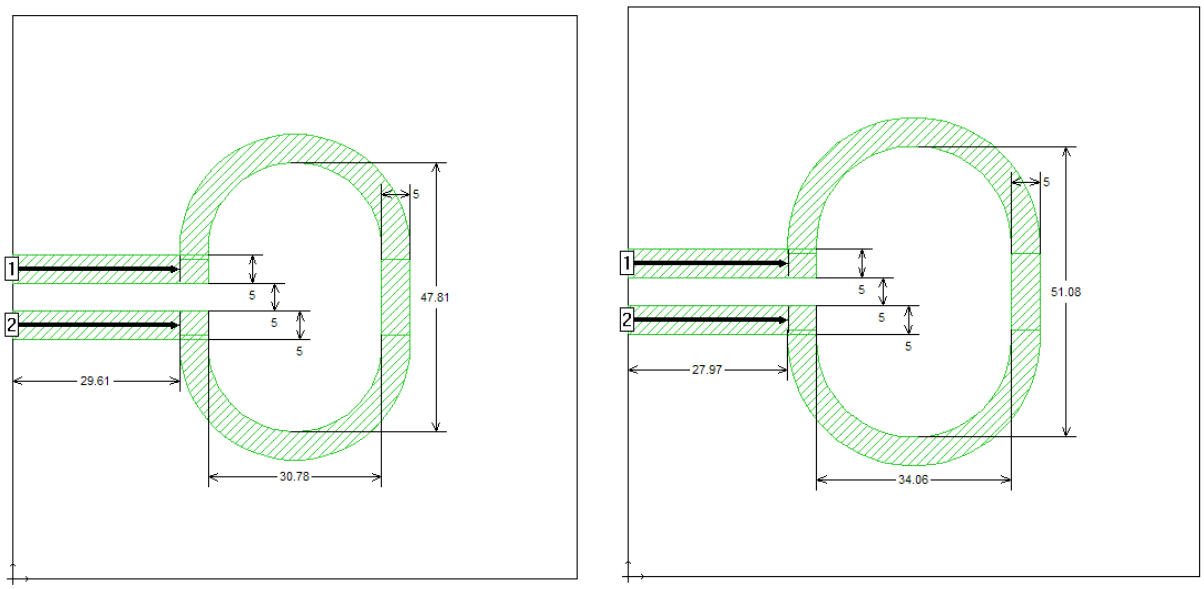


(a) (b)

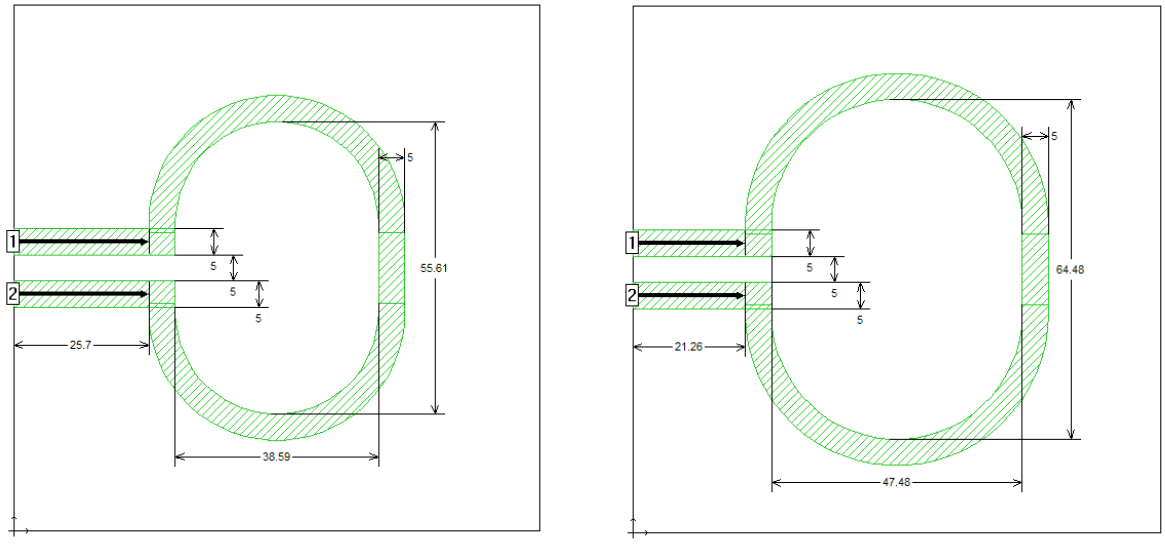


(c) (d)

**Figure 3.** 2D layout of (a) 68 pH, (b) 75 pH, (c) 84.7 pH and (d) 104 pH inductors along with their respective dimensions. Note that the inner radii are half of the horizontal diameters of the respective inductors.

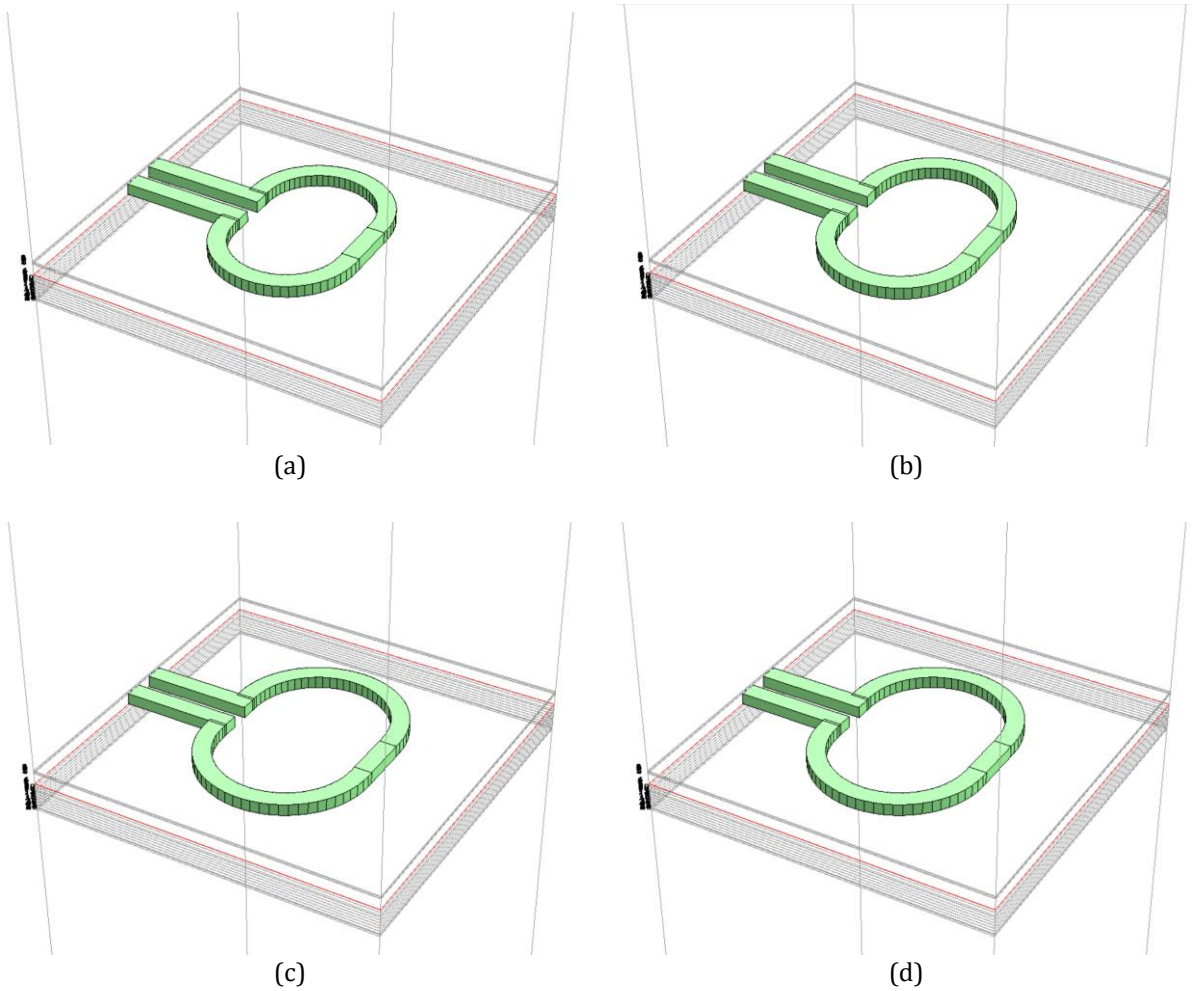

(a) (b)

(c) (d)

**Figure 4.** 3D layout of (a) 68 pH, (b) 75 pH, (c) 84.7 pH and (d) 104 pH inductors with complete process layer from Silterra.

A close view of the inductance curves when they are operating within ±0.2 pH of their targeted values are depicted in Figure 5. The figure reveals that $L_p$ (68 pH), $L_s$ (75 pH), $L_g$ (84.7 pH) and $L_d$ (104 pH) have operating bandwidths of 9.5 GHz, 8.5 GHz, 4 GHz and 1.5 GHz, respectively. The results infer that the bandwidth of the inductors decreases as the inductance value increases.

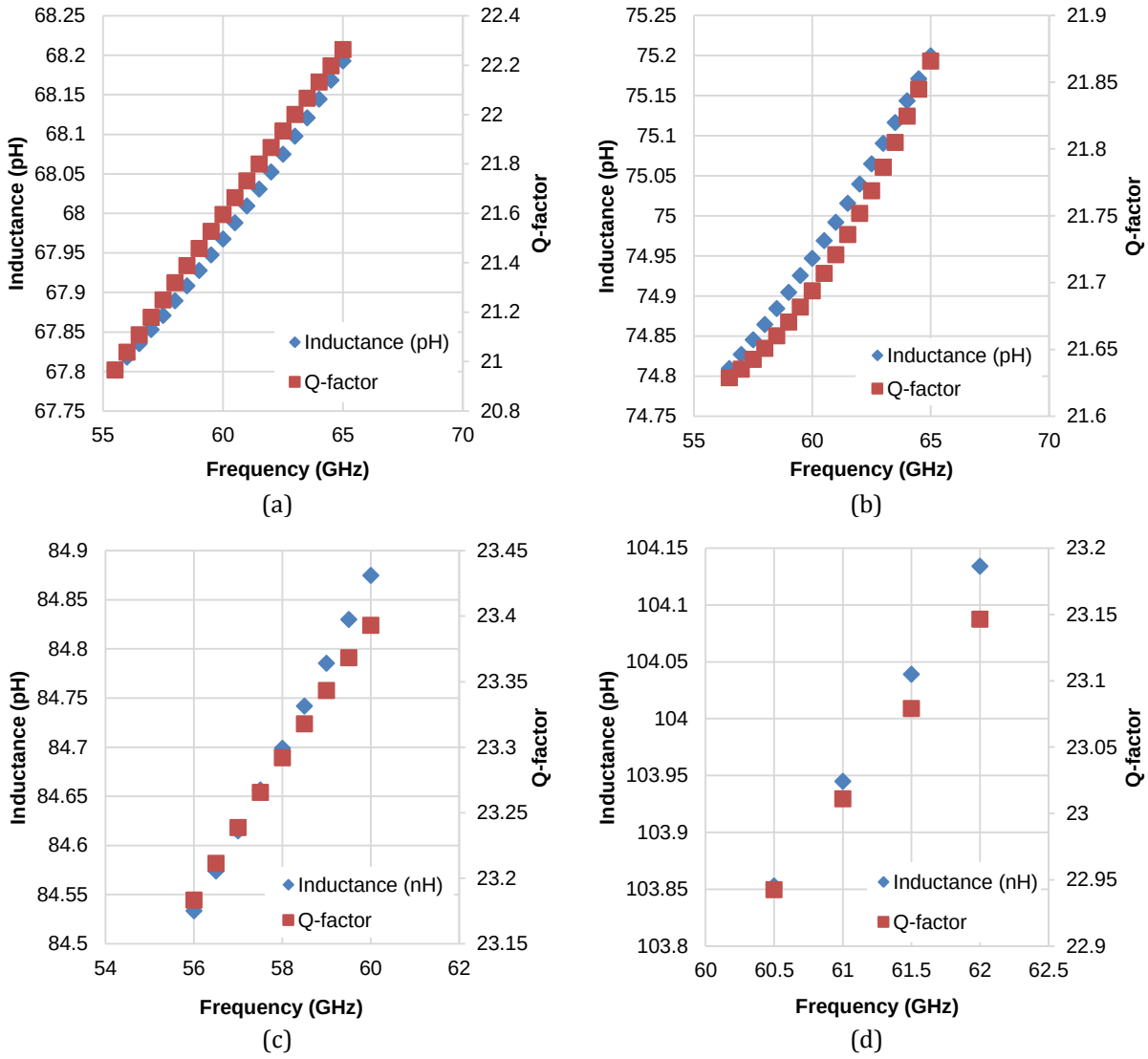


**Figure 5.** Simulated inductances and Q-factors of (a) $L_p$ (68 pH), (b) $L_s$ (75 pH), (c) $L_g$ (84.7 pH) and (d) $L_d$ (104 pH) inductors at their respective operating frequencies.

Figure 6 shows the simulation results for the four inductors. As can be clearly seen from the figure, the inductances decrease until about 40 GHz before they start to increase exponentially. The Q-factors, on the other hand, generally increase beyond 100 GHz before they start to decrease. It can also be observed from Figure 6 and Table 2 that the designs for the four inductors perform very well at the vicinity of 60 GHz – their inductance values fall close to their targeted values; while their Q-factors are all above 20.

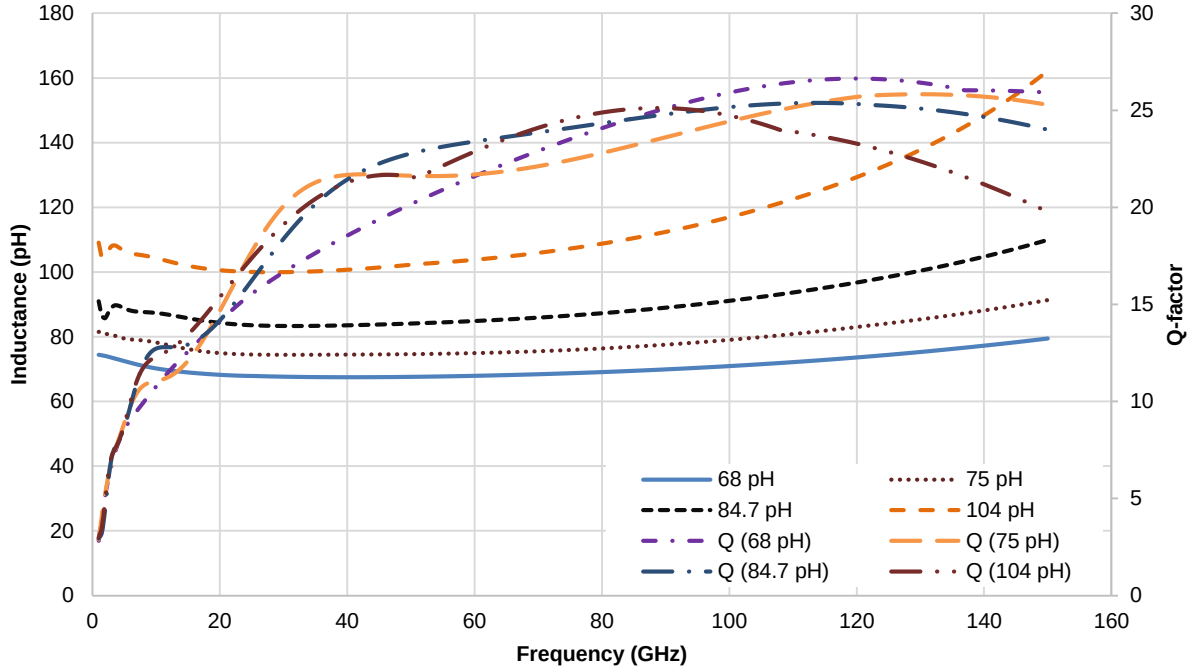


**Figure 6.** Simulated inductances of the four spiral inductor designs and their respective Q-factors from 1 GHz to 150 GHz.

**Table 2** Parameters of inductors after simulations

| Inductor | Target Inductance (pH) | Inner Radius ($\mu$m) | Simulated Inductance at 60 GHz (pH) | Simulated Q-factor at 60 GHz |
|---|---|---|---|---|
| $L_p$ | 68 | 15.39 | 67.97 | 21.6 |
| $L_s$ | 75 | 17.03 | 74.95 | 21.69 |
| $L_g$ | 84.7 | 19.295 | 84.87 | 23.39 |
| $L_d$ | 104 | 23.74 | 103.8 | 22.87 |

## 5. CONCLUSION

The structures of four spiral inductors intended to be applied in a 60 GHz CMOS LNA were designed and synthesised. The results show that the targeted inductances exhibit a minimum operating bandwidth of 1.5 GHz with Q-factors more than 20. The design structures also show that single-turn spiral inductors could be employed to realise inductances below 110 pH. The designs abide the Silterra's CL130G foundry-specific data and script files hence could be incorporated into the PDK.

## ACKNOWLEDGEMENTS

The authors would like to thank the staffs in Silterra modelling team for disclosing the classified technical details of the process layer. The information provided by the team members is very valuable in improving the accuracy of the simulations.

**REFERENCES**

[1] M. Božanić & S. Sinha, Millimeter- Wave Low Noise Amplifiers. Springer, (2018).
[2] A. Scuderi, E. Ragonese, T. Biondi & G. Palmisano, Integrated Inductors and Transformers, (2010).
[3] C. L. Chua, D. K. Fork, K. Van Schuylenbergh & J. P. Lu, "Out-of-plane high-Q inductors on low-resistance silicon," J. Microelectromechanical Syst. **12**, 6 (2003) 989–995.
[4] N. C. Schirmer, J. Hesselbarth, S. Ströhle, B. R. Burg, M. K. Tiwari & D. Poulikakos, "Millimeter-wave on-chip solenoid inductor by on-demand three-dimensional printing of colloidal nanoparticles," Appl. Phys. Lett. **97**, 24 (2010) 2–5.
[5] C. P. Yue & S. S. Wong, "On-chip spiral inductors with patterned ground shields for si-based RF IC's," IEEE J. Solid-State Circuits **33**, 5 (1998) 118–126.
[6] A. Sahu, B. Grayczyk, M. Almalkawi, V. Devabhaktuni & P. Aaen, "High-Q spiral inductors with multilayered split-ring resonator (SRR) patterned ground shields," in IEEE Antennas and Propagation Society, AP-S International Symposium (Digest), (2014) 346–347.
[7] J. Luo, J. He, H. Wang, S. Chang, Q. Huang & X. P. Yu, "A 28 GHz LNA using defected ground structure for 5G application," Microw. Opt. Technol. Lett. **60**, 5 (2018) 1067–1072.
[8] N. S. Yusof *et al.,* "Electronic controlled CMOS inductor with patterned metal ground shields for fine inductance tuning application," Indones. J. Electr. Eng. Comput. Sci. **14**, 2 (2019) 937–948.
[9] M. S. Amran, Q. L. S. Imm & A. V. Kordesch, "Design of a 130nm CMOS differential cross-coupled 5 GHz LC oscillator," in 2005 Asia-Pacific Conference on Applied Electromagnetics, APACE 2005 - Proceedings, 2005 (2005) 242–244.
[10] M. H. M. Ali, C. L. Ler, S. C. Rustagi, Y. M. Yusof, N. D. Arora & B. Y. Majlis, "The impact of electromagnetic coupling of guard ring metal lines on the performance of on-chip spiral inductor in silicon CMOS," Proc. 2nd Asia Symp. Qual. Electron. Des. ASQED 2010, **1** (2010) 285–288.
[11] S. A. Z. Murad, M. F. Ahamd, M. M. Shahimin, R. C. Ismail, K. L. Cheng & R. Sapawi, "High efficiency CMOS Class e power amplifier using 0. 13 μm technology," IEEE Symp. Wirel. Technol. Appl. ISWTA, (2012) 85–88.
[12] M. H. Hamzah, A. B. Jambek & U. Hashim, "Design and analysis of a two-stage CMOS op-amp using Silterra's 0.13 μm technology," ISCAIE 2014 - 2014 IEEE Symp. Comput. Appl. Ind. Electron. (2015) 55–59.
[13] A. Azizan, S. A. Z. Murad, M. M. Ramli & R. C. Ismail, "Design of a 2.4 GHz CMOS LNA using two-stage forward body bias technique for WSN application," 2015 IEEE Student Conf. Res. Dev. SCOReD 2015, (2015) 415–417.
[14] S. Rasidah, M. H. S. Maisurah, E. F. Nazif, K. Norhapizin & A. I. A. Rahim, "The design of ground shield spiral inductor using 0.13 μm CMOS technology for millimeter-wave radio over fiber applications," RSM 2015 - 2015 IEEE Regional Symposium on Micro and Nano Electronics, Proceedings, (2015).
[15] F. Eshghabadi, F. Banitorfian, N. Mohd Noh, M. T. Mustaffa & A. Abd Manaf, "Post-process die-level electromagnetic field analysis on microwave CMOS low-noise amplifier for first-pass silicon fabrication success," Integr. VLSI J. **52** (2016) 217–227.
[16] M. M. Harsoori & T. Z. A. Zulkifli, "60 GHz microstrip filter in 0.13μm RF CMOS technology," Proc. - 14th IEEE Student Conf. Res. Dev. Adv. Technol. Humanity. SCOReD 2016, (2017).
[17] M. M. Harsoori, T. Z. A. Zulkifli, U. Abbas & S. Sattar, "A gain boosting single stage cascode LNA for millimeter-wave applications," Asia Pacific Conf. Postgrad. Res. Microelectron. Electron., vol. 2017-October, (2018) 109–112.
[18] Sonnet Software Inc., "Sonnet® User's Guide." Sonnet Software Inc., Syracuse, NY, USA, (2018).
[19] A. F. Horn, P. A. Lafrance, C. J. Caisse, J. P. Coonrod & B. B. Fitts, "Effect of conductor profile structure on propagation in transmission lines," Designcon, (2016).
[20] Y. E. Ozmen & T. Imeci, "Spiral patch antenna at 12 GHz," 2017 Int. Appl. Comput. Electromagn. Soc. Symp. - Italy, ACES 2017, (2017) 12–13.

[21] G. Djengomemgoto, R. Altunok, C. Karabacak, S. T. Imeci & T. Durak, "Dual-band gemini-shaped microstrip patch antenna for C-band and X-band applications," 2017 Int. Appl. Comput. Electromagn. Soc. Symp. - Italy, ACES 2017, (2017) 5–6.
[22] A. Elakaş, G. A. Imrak, M. Şencan, S. T. Imeci & T. Durak, "Microstrip patch antenna with triangular slits," 2018 Int. Appl. Comput. Electromagn. Soc. Symp. Denver, ACES-Denver 2018, (2018) 12–13.
[23] M. E. Koca, T. Durak & S. T. Imeci, "Roof shaped rectangular slotted patch antenna at 18.3 GHz," 2018 Int. Appl. Comput. Electromagn. Soc. Symp. Denver, ACES-Denver 2018, (2018) 1–2.
[24] E. Thae Aye & N. Chaw Myat, "Rectangular Microstrip Patch Antenna Array for RFID Application Using 2.45 GHz Frequency Range," Int. J. Sci. Res. Publ. **4**, 6 (2014) 1–7.
[25] S. S. Mohan, M. D. M. Hershenson, S. P. Boyd & T. H. Lee, "Simple accurate expressions for planar spiral inductances," IEEE J. Solid-State Circuits **34**, 10 (1999) 1419–1420.